IEEE Access
Multidisciplinary | Rapid Review | Open Access Journal

Received April 16, 2022, accepted May 1, 2022, date of publication May 12, 2022, date of current version May 18, 2022.

Digital Object Identifier 10.1109/ACCESS.2022.3174652

Performance Analysis of Block/Zero-Comb Pilot and Nonzero-Comb Pilot Over MIMO-PLC Systems

SHIRUI ZHANG AND CHARALAMPOS C. TSIMENIDIS, (Senior Member, IEEE)
School of Engineering, Newcastle University, Newcastle Upon Tyne NE1 7RU, U.K.

Corresponding authors: Shirui Zhang (s.zhang19@ncl.ac.uk) and Charalampos C. Tsimenidis (charalampos.tsimenidis@ncl.ac.uk)

This work was supported by the Engineering and Physical Sciences Research Council (EPSRC) under Grant EP/R002665/1.

ABSTRACT In this paper, we consider Power Line Communications (PLC) for Smart Grid (SG) using Multiple-Input Multiple-Output and Orthogonal Frequency Division Multiplexing (MIMO-OFDM). We investigate a 2×2 MIMO-OFDM system and propose a novel nonzero comb pilot (NZCP) design for channel estimation that can cope with pilot contamination without the need for zero-pilot insertion in adjacent channels. The Bit Error Rate (BER) performance vs. E_b/N_0 is demonstrated using numerical simulations for uncoded and coded systems using Low Parity Density Check (LDPC) error correcting codes. The performance is compared with conventional Zero-comb pilot (ZCP) and the block pilot methods through frequency-selective multipath PLC channels and in the presence of Additive White Gaussian Noise (AWGN) and symmetric α-stable (SαS) type of impulsive noise. Additionally, a novel averaging method is introduced to reduce the effects of AWGN, SαS and Mean Square Error (MSE) metric is used to assess the quality of the channel estimation. The numerical results presented demonstrate that the NZCP approach using averaging outperforms all the methods considered, e.g. for the uncoded system at a BER of 10^{-5} an improvement in E_b/N_0 of 3.6 and 4 dB against ZCP and block approaches, respectively. In contrast, in the coded system, the coding gain is of the order of 20 dB compared to the uncoded cases with the NZCP proposed method outperforming all the other considered approaches by at least 0.5 dB. Furthermore, the presented BER results demonstrate that the SαS impulsive noise has a greater impact on the performance of the MIMO-PLC system. It is shown that when utilizing a hardlimiter to limit the effects of SαS, the BER can reach 8×10^{-5} at an E_b/N_0 of 45 dB when $\alpha = 1.5$. In contrast, when $\alpha = 1$, which represents a more severe case of SαS, a BER level of 3.5×10^{-4} is attained at an E_b/N_0 of 90 dB. However, the proposed averaging-NZCP system can robustly estimate the channel frequency responses (CFR) of the MIMO-PLC channel over SαS noise outperforming other commonly used pilot approaches.

INDEX TERMS MIMO-PLC, channel estimation, comb/block pilot, averaging comb pilot, nonzero comb pilot.

I. INTRODUCTION

High-speed Power-Line Communications (PLC) over electrical power lines has been standardized in 2010 via the IEEE 1901 [1] standard often referred to as Broadband over Power Lines (BPL). The power line channel is a challenging propagation medium for communications, however, its low cost of operation for smart grid applications has made it the subject of a vast body of research [2]. Over the past 10 years, Multiple-Input Multiple-output (MIMO) BPL techniques have been considered and researched extensively for the PLC channel in order to increase transmission speeds closer to the available channel capacity [3]–[8].

MIMO is the primary technology in the fourth and fifth-generation (4G/5G) of wireless communication [9]. In the PLC channel, the domestic electrical wiring includes three types of wires: Phase (P), Neutral (N) and Protective Earth (PE). In Single-Input Single-Output (SISO) systems, the communication signals are transmitted via the P and N wires using Time-division Multiple Access (TDMA) and Carrier-sense multiple access with collision avoidance (CSMA/CA). However, voltage differences between PE,

The associate editor coordinating the review of this manuscript and approving it for publication was Luyu Zhao.

P and N as well that can be utilized to establish MIMO communications using the three ports, i.e. P-PE, PE-N and P-N, to implement 3 × 3 MIMO system, implying 3 transmitters and 3 receivers per terminal [8]. The advantages and problems of MIMO-PLC systems have been discussed extensively in [10]–[11], where appropriate communication methods have been proposed and investigated.

A. RELATED WORK

To accurately recover the transmitted signal at the receiver, it is necessary to estimate the impulse and/or frequency responses of the PLC channel. This estimation process is affected by the noise of electrical equipment operating on the power lines and has a serious impact on the performance of BPL systems. Thus, a high-quality channel estimation method design is essential for MIMO Orthogonal Frequency Division Multiplexing (OFDM) systems using the PLC channel. Previous research focused on pilot design to improve the performance of SISO or MIMO channel estimation systems. According to [12], Song used comb type pilot to estimate STBC-OFDM SISO system. The STBC method gives different value of pilot in different space and time position. Compare with the zero-comb pilot (ZCP) system, STBC does save the capacity to transmit the information data and it suits the MIMO system as well, but the BER performance is not good. The Mean Square Error (MSE) is just −10 dB when the Signal-to-Noise Ratio (SNR) is 9 dB. That means there is huge difference between perfectly known CFR and estimated CFR. In 2018, Liu presented a new proposed preamble design based on comb pilot in Filter Bank Multicarrier with Offset Quadrature Amplitude Modulation (FBMC/OQAM) [13] for MIMO system. The best *MSE* performance of this method is about −20 dB when SNR is 9 dB which is not good enougy. Hou presented a new Superimposed comb type pilot design to consider the MIMO-OFDM system as several SISO-OFDM channels to avoid channel interference [14]. The performance of this comb pilot method is better than before with the value of *MSE* is about −18 dB when the SNR is 8 dB by using QPSK modulation under $\frac{1}{3}$ pilot to information data ratio. Moreover, in 2018 [15], Takuya utilized Walsh-Hadamard and null pilots for channel estimation MIMO system with Advanced Television Systems Committee (ATSC) 3.0, which is the last digital terrestrial television (DTT) standard. These research works represent examples of pilot design methods. Furthermore, pilot contamination is a key problem that needs to be solved. Fuqian investigated the pilot contamination in massive MIMO systems. They proposed different pilot decontamination methods for both Time-Domain Multiplexing (TDM) and Frequency-Domain Multiplexing (FDM) based pilots, and demonstrated their performance [16].

B. CONTRIBUTION

In this paper, we focus on channel estimation methods of 2 × 2 MIMO-PLC systems shown in Fig. 1 that utilize real-valued OFDM waveforms. The contribution of the paper can be summarized as follows. Firstly, the proposed new channel estimation method, referred to as Nonzero-comb Pilot (NZCP), is introduced that estimates the underlying MIMO channels in two time slots. To solve the four unknown channel gains per subcarrier in frequency domain, the 2 × 2 MIMO system requires a set of four independent linear equations. Thus, for every two time slots, the unknown channel gains can be estimated by solving the system of four equations at the pilot positions and then performing interpolation to obtain the CFR at the data subcarriers. The proposed novel NZCP in this paper does not require zero pilot insertion in adjacent MIMO channels to avoid pilot contamination. Therefore, the channel capacity of NZCP is increased compared to the traditional ZCP system. In contrast, the ZCP approach requires insertion of zero pilots in adjacent MIMO channels to avoid pilot contamination. Therefore, when these two systems transmit the same amount of pilot symbols, the pilot gap of the ZCP is the twice as long compared to the NZCP. Thus, the NZCP approach outperforms ZCP in terms of MSE and BER performances. Furthermore, we introduce weighted CFR averaging that further improves the performance of both ZCP and NZCP significantly.

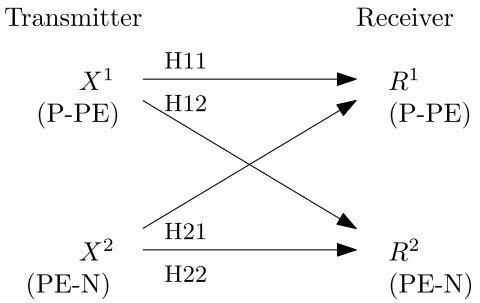

FIGURE 1. 2 × 2 MIMO-PLC model.

C. ORGANIZATION OF PAPER

The remainder of the paper is organized as follows: Section II presents the system model, including the real-valued OFDM and PLC model. Section III introduces two channel estimation methods, i.e. comb and block pilot for the SISO and MIMO-OFDM BPL system under consideration. Section IV presents a novel averaging comb pilot method with the zero and nonzero adjacent pilots. Numerical results are shown in Section V to evaluate the performance of the proposed channel estimation techniques. Finally, we summarize this paper in Section VI.

II. SYSTEM MODEL

A. OFDM INPUT SIGNAL

As can be seen in Fig. 7, after the Quadrature Amplitude Modulation (QAM), interleaver and Hermitian symmetry (HS) is imposed on all modulated subcarriers in frequency domain in order to obtain a real-valued OFDM symbol, that is,

$$X_n^\tau = [\mathrm{Re}\{D_0^\tau\},\ D_k^\tau,\ \mathrm{Im}\{D_0^\tau\},\ (D_{N_k-k}^\tau)^*], \quad (1)$$

$$X_k^\tau = (X_{N-k}^\tau)^*, \quad (2)$$

where Re{ } and Im{ } denote the real and imaginary operators, ( )* is the complex-conjugate operator, $N = 4096$ represents the number of OFDM symbol subcarriers and $n = 0, 1, \ldots, N-1$ represents the index of subcarrier. The length of the QAM signal D_k^τ is $N_k = \frac{N}{2}$ and $k = 0, 1, \ldots, N_k - 1$ denotes the index number [2]. $\tau = \{1, 2\}$ denotes the index of transmitter. After Inverse Fast Fourier Transform (IFFT), the OFDM input signal in time domain x_n^τ became into real-valued. To eliminate the Inter-Symbol-Interference (ISI) between the OFDM symbols, the cyclic prefix (CP), which is designed to outstrip the maximum PLC channel delay spread, is inserted at the beginning of each time domain OFDM symbol by copying the last N_{cp} samples of the OFDM symbol x_n^τ to obtain the real-valued OFDM symbol in time domain $\mathbf{x}^\tau = [x_{N-N_{cp}}^\tau, x_{N-N_{cp}+1}^\tau, \ldots, x_{N-1}^\tau, x_0^\tau, \ldots, x_{N-1}^\tau]$ before passing through the PLC channel.

B. SISO PLC CHANNEL MODEL

The multipath PLC channel utilized in this paper is shown in Fig. 2 [17], [18]. The OFDM signal is transmitted from point A to the receiver end at point F. However, due to multipath propagation several possible paths are established, i.e. $A \to B \to D \to F, A \to B \to C \to B \to D \to F, A \to B \to D \to E \to D \to F, A \to B \to C \to B \to D \to E \to D \to F$. The channel frequency response (CFR) for this channel can be given as [19]

$$H(f) = \sum_{i=1}^{L} \underbrace{g_i}_{\text{weighting factor}} \underbrace{e^{-(a_0 + a_1 f^q) d_i}}_{\text{attenuation}} \underbrace{e^{-j2\pi f \frac{d_i}{v_p}}}_{\text{delay}}, \tag{3}$$

where L is the number of multipath, a_0 and a_1 are the attenuation parameters, g_i is the weighting factor of the multipath PLC channel, q is the exponent of attenuation factor, d_i is length of the cable, and v_p is the phase velocity given as

$$v_p = \frac{c_o}{\sqrt{\varepsilon_r}}, \tag{4}$$

where c_0 denotes the speed of light, which is 3.0×10^8 m/s, and ε_r is the dielectric constant of the insulation material. In general, polyethylene is the most commonly used power line insulation material for which the dielectric constant is 4. The channel impulse response (CIR) is obtained by using the inverse Fourier transform of (3). For $q = 1$, it is shown in the appendix to be

$$\begin{aligned} h(t) &= \frac{1}{B} \sum_{i=1}^{L} g_l e^{-a_0 d_i} u(t - t_i) \\ &\times \frac{\cos(\phi_i)[1 - e^{-a_1 d_i B} \cos(\theta_i)] + e^{-a_1 d_i B} \sin(\phi_i) \sin(\theta_i)}{\sqrt{(a_1 d_i)^2 + [2\pi(t - t_i)]^2}} \end{aligned} \tag{5}$$

where B is the signal bandwidth, $\phi_i = \tan^{-1}\left(\frac{2\pi(t-t_i)}{a_1 d_i}\right)$ and $\theta_i = 2\pi B(t - t_i)$. The truncated and energy-normalized CIR is illustrated in Fig. 3. Truncation is performed to remove trailing zeros as the CIR values become very small after $L = 200$. Furthermore, it is worth noting that the variable t denotes the multipath delay spread of the PLC channel in units of seconds, and that the multipath amplitudes have been normalized so that $\sum_{t=0}^{L-1} |h(t)|^2 = 1$.

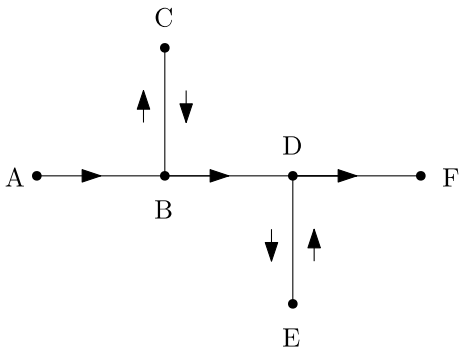

FIGURE 2. Multipath signal propagation in one-tap cables.

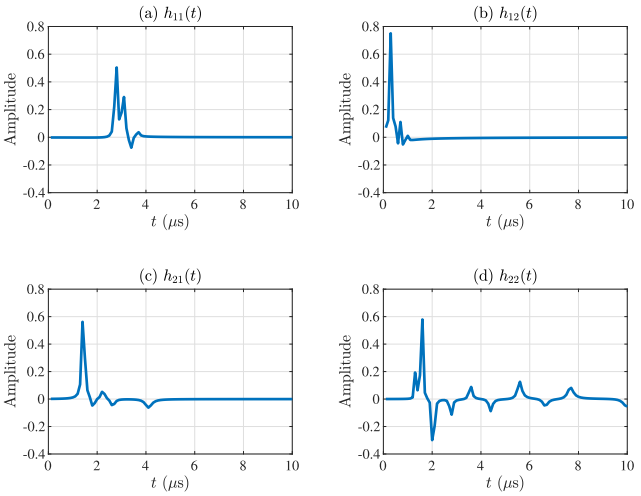

FIGURE 3. The truncated and energy-normalized CIRs of a 2 × 2 MIMO-PLC.

C. MIMO-PLC MODEL

In this paper, four different number of path and parameter value of the PLC channels have been utilized to simulate a 2 × 2 MIMO-OFDM PLC-based system. The amplitude of the four CIRs and the magnitude of the four CFRs of the MIMO-PLC channels are illustrated in Fig. 3 and Fig. 4.

After CP removal and FFT operation, the received signal at the n-th subcarrier can be given as

$$\mathbf{R}_n = \mathbf{H}_n \mathbf{X}_n + \mathbf{W}_n \tag{6}$$

where $\mathbf{R}_n \in \mathbb{C}^{2\times 1}$ is the received signal vector, $\mathbf{H}_n \in \mathbb{C}^{2\times 2}$ is the frequency-domain, channel coefficient matrix, and $\mathbf{W}_n^{2\times 1}$ is the vector of the zero-mean, additive white Gaussian noise samples with variance σ_W^2, i.e. $\mathcal{N}(0, 2\sigma_W^2)$.

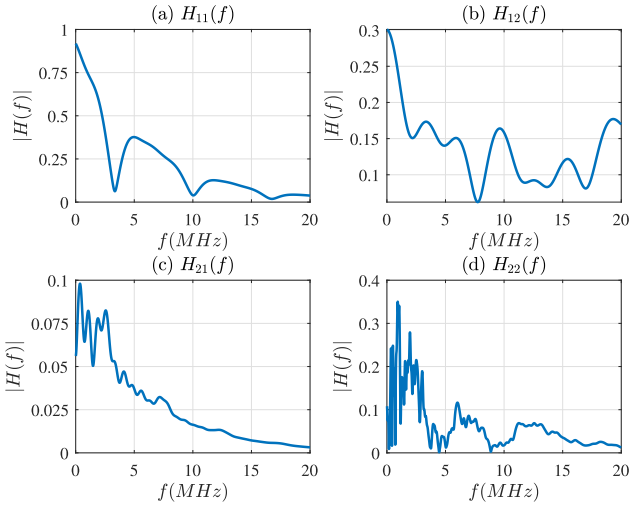

FIGURE 4. The magnitude of channel frequency response of a 2 × 2 MIMO-PLC.

To estimate the four CFRs of the 2 × 2 MIMO-PLC channel, we will consider two approaches. i.e. the block and comb pilot methods.

D. SαS DISTRIBUTION NOISE

In practice, the impulsive noise generated by electromagnetic pulse radiation and high frequency electrical equipment will have a great impact on the performance of a PLC system. Thus, in this paper, we will investigate the impact of joint effect of AWGN and SαS noise on the BER performance.

We consider SαS type of impulsive noise distribution with a skewness parameter $\beta = 0$. The characteristic function of symmetric SαS is given as

$$\varphi(t) = \exp\left(j\delta t - \gamma^{\alpha} \mid t \mid^{\alpha}\right). \tag{7}$$

Hence, the probability density function (PDF) of the SαS distribution noise model can be defined as [21]

$$p_{\alpha}(x;\delta;\gamma) = \frac{1}{2\pi}\int_{-\infty}^{\infty} \exp(j\delta t - \gamma^{\alpha}|t|^{\alpha})e^{-jtx}dt. \tag{8}$$

The range of α is $0 < \alpha \leq 2$, however, when $\alpha = 1$, we obtain the Cauchy distribution, whose PDF given as

$$p_1(x;\delta,\gamma) = \frac{1}{\pi}\frac{\gamma}{\gamma^2 + (x-\delta)^2}. \tag{9}$$

In contrast, when $\alpha = 2$, the distribution is Gaussian and the standard PDF is

$$p_2(x;\delta,\gamma) = \frac{1}{2\sqrt{\pi}\gamma}\exp\left[-\frac{(x-\delta)^2}{4\gamma^2}\right]. \tag{10}$$

According to Juan in [20], the geometric power of the SαS variable is given by

$$S_0 = \frac{(C_g)^{\frac{1}{\alpha}}\gamma}{C_g}, \tag{11}$$

where $C_g = 1.78$ is the exponential of the Euler constant and the γ is the dispersion, which is related to the variance σ^2 as $\sigma^2 = 2\gamma^2$. With the amplitude of the modulation signal A, the Geometric Signal-to-Noise Ratio can be defined as

$$SNR_G = \frac{1}{2C_g}\left(\frac{A}{S_0}\right)^2. \tag{12}$$

The SNR $\frac{E_b}{N_0}$ is defined as [21]

$$\frac{E_b}{N_0} = \frac{SNR_G}{2R_c} = \frac{1}{4C_gR_c}\left(\frac{A}{S_0}\right)^2. \tag{13}$$

For M-ary modulation, the SNR $\frac{E_b}{N_0}$ is given by

$$\frac{E_b}{N_0} = \frac{1}{4C_gR_c\log_2(M)}\left(\frac{A}{S_0}\right)^2, \tag{14}$$

where $A^2 = E_s$. Combining (11) and (14), the dispersion γ is given by

$$\gamma = \sqrt{\frac{E_sC_g}{4C_g^{\frac{2}{\alpha}}R_c\log_2(M)\frac{E_b}{N_0}}}, \tag{15}$$

III. CHANNEL ESTIMATION MODEL IN SISO AND MIMO SYSTEM

Channel estimation refers to methods that identify the channel impulse and/or frequency responses of communications channel. For OFDM systems, two methods are widely used, i.e., the comb and block pilot approaches, which are considered as non-blind estimation methods as they utilize a reference signal. Although the pilots occupy information bits and waste bandwidth, non-blind estimation is widely utilized because of its excellent performance compared to blind methods and their low-complexity of operation [22].

A. BLOCK PILOT APPROACH IN SISO/MIMO SYSTEM

Assume that the ratio of the number of pilot to the number of information data is $\frac{1}{8}$, in other word, the length of the OFDM data block, $N_b = 9$ can be considered in nine OFDM symbols - one OFDM symbol is full of pilots and eight OFDM symbols are the information data, which can be expressed in Fig. 5 (a) [23], [24]. N_m denotes the number of OFDM symbols with a multiple of eight of size in this paper. The transmitter can send one pilot symbol in each OFDM data block as the tracking data in all OFDM subcarriers to the receiver to calculate the estimated channel frequency response in SISO-PLC system. In this instance, the total number of the OFDM input symbols should be $\frac{9}{8}N_m$.

In the block pilot approach illustrated in Fig. 5 (a), the 2 × 2 MIMO-PLC can be treated as four independent SISO-PLC channels. They can be estimated by transmitting two consecutive pilot blocks, that is, one per transmitter. When the 1st transmitter is activated, H_n^{11} and H_n^{21} can be estimated, while H_n^{12} and H_n^{22} are obtained when the 2nd transmitter is operated. In this way, the cross-channel interference is avoided. The received signal at the n-th subcarrier and ρ-th receiver can be given as

$$R_n^{1,\rho} = X_n^{1,\rho}H_n^{1,\rho} + W_n^{1,\rho}, \tag{16}$$

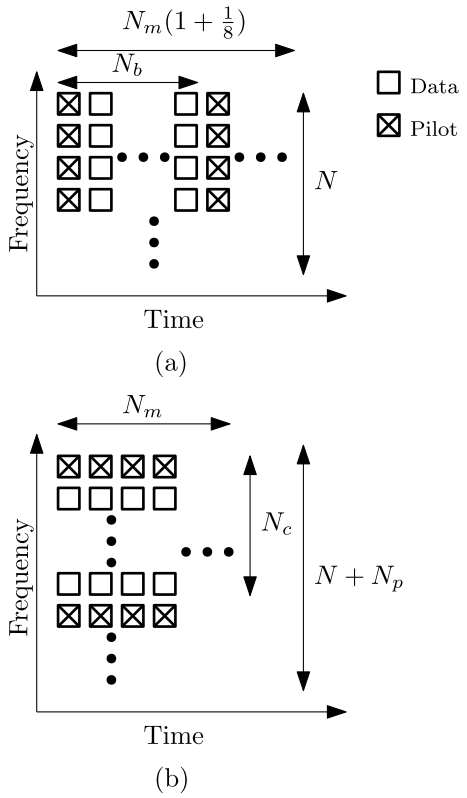

FIGURE 5. Types of SISO channel estimation: (a) Block Pilot, (b) Comb Pilot.

$$R_n^{2,\rho} = X_n^{2,\rho} H_n^{2,\rho} + W_n^{2,\rho}, \tag{17}$$

where $R_n^{1,\rho}$ and $R_n^{2,\rho}$ are the received samples of the block pilot system. $\rho = 1, 2$ represents the index of the receiver. $W_n^{\tau,\rho}$ denotes the noise channel, $H_n^{\tau,\rho}$ is the CFR coefficient of the n-th subcarrier of the 2×2 MIMO-PLC channel matrix and $X_n^{\tau,\rho}$ is the input block pilot OFDM symbol in the frequency domain. For the n-th subcarrier, the estimated CFR matrix elements of the block pilot MIMO-PLC system can be estimated as

$$\begin{aligned} \hat{H}_n^{\tau,\rho} &= \frac{R_n^{\tau,\rho}}{X_n^{\tau,\rho}} \\ &= \frac{X_n^{\tau,\rho} H_n^{\tau,\rho} + W_n^{\tau,\rho}}{X_n^{\tau,\rho}}. \\ &= H_n^{\tau,\rho} + \frac{W_n^{\tau,\rho}}{X_n^{\tau,\rho}}. \end{aligned} \tag{18}$$

B. COMB PILOT APPROACH IN SISO/MIMO SYSTEM

Under the same circumstance of the block pilot approach, in each nine subcarriers ($N_c = 9$), we use one subcarrier to transmit pilot to make the ratio of pilot to information data is $\frac{1}{8}$, which shows in Fig. 5 (b) [23], [25]. The total length of the subcarriers should be included both the original number of subcarriers ($N = 4096$) and number of pilot ($N_p = \frac{N}{8} = 512$). At the receiver end, the estimated CFR in pilot position subcarriers can be calculated. Moreover, the rest of the remaining subcarriers' estimated CFR can be calculated accurately by using the interpolation algorithm [26]. To be more concrete, the interpolation cubic spline model, which is described in [27], has been constructed to create the estimated CFR in both ZCP and NZCP approach.

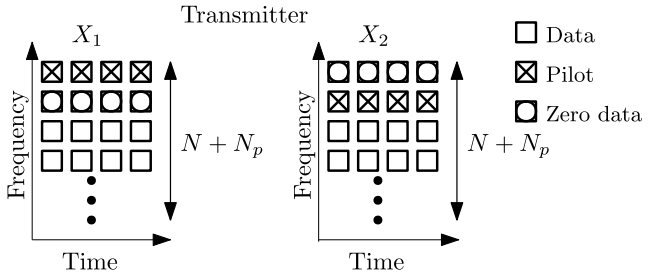

FIGURE 6. ZCP model.

Compared with the traditional SISO system, the Channel State Information (CSI) estimation in the MIMO system is more difficult because the signal received on any subcarriers is the superposition of multiple distorted signals due to various devices. The pilot sequences transmitted by different devices need to be orthogonal to each other in the MIMO system. Otherwise, the receiver cannot distinguish each pilot, which results in pilot pollution and leads to inaccurate channel estimation. The time gap, which can be staggered in time, allowing only one device to transmit data at a specific time, has been demonstrated [28].

In [29], Lavafi presented a zero-comb pilot method to estimate channel frequency domain, which is illustrated in Fig. 6. In this paper, the ZCP method used as a reference method to compare to our proposed channel estimation method. In this method, in order to avoid pilot contamination, whenever a comb-pilot symbol is added at a subcarrier of a transmitter, a zero subcarrier is added to the subcarrier of adjacent MIMO transmitters. Because the zero subcarrier does not transmit any information data, it can be regarded as pilot subcarrier as well. Clearly, this approach can only be efficient with small-sized MIMO systems and becomes impractical with dimensions larger than 3×3.

At subcarrier level, the ratio of pilot (with number of zero data) and information data should be $\frac{1}{8}$ as well. Assume that the number of pilots is the same as the number of zero data, the length of the QAM symbol subcarrier with pilot should be $N_k + \frac{1}{2}N_p$. The pilot symbols are interleaved with QAM symbols to produce $\mathbf{D}^\tau \in \mathbb{C}^{1\times(N_k+\frac{1}{2}N_p)}$ as

$$\begin{aligned} \mathbf{D}^1 = [&P_0, 0, D_0, \ldots, D_{15}, P_1, 0, \ldots, \\ &P_{N_p-1}, 0, D_{N_k-16}, \ldots, D_{N_k-1}], \end{aligned} \tag{19}$$

$$\begin{aligned} \mathbf{D}^2 = [&0, P_0, D_0, \ldots, D_{15}, 0, P_1, \ldots, \\ &0, P_{N_p-1}, D_{N_k-16}, \ldots, D_{N_k-1}], \end{aligned} \tag{20}$$

We have assumed here arbitrarily that the same value $P_i = P$ is used for all pilots and the pilot spacing, which is 16, with one pilot and one zero data to make the ratio of the number of pilot to information data is $\frac{1}{8}$. The OFDM symbol, which

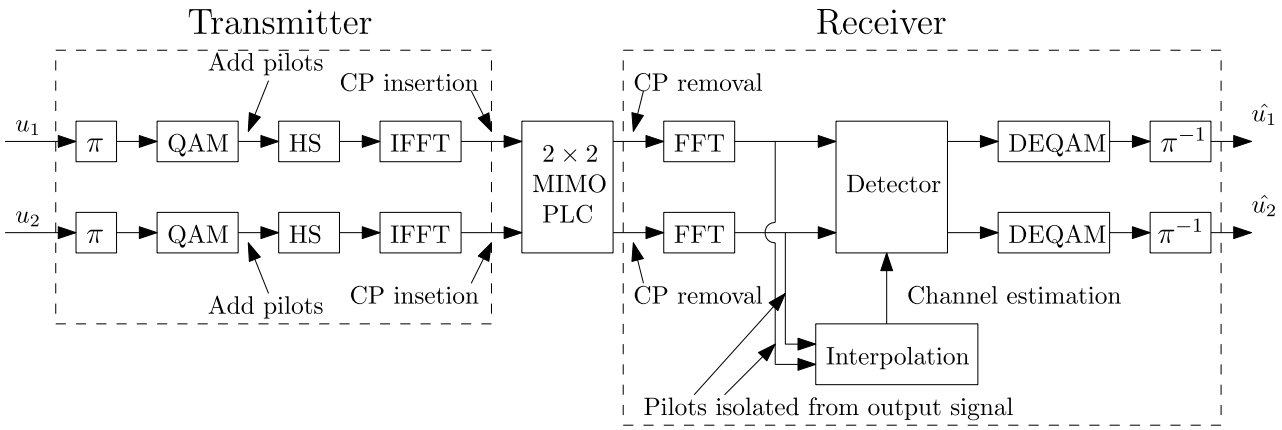

FIGURE 7. Proposed channel estimation system model.

the length of subcarriers is doubled because of applying Hermittian symmetry in (1), in frequency domain with pilots included, $\mathbf{X}^{\tau} \in \mathbb{C}^{1\times(N+N_p)}$ can be given as

$$\begin{aligned}\mathbf{X}^1 &= [\mathrm{Re}\{P\}, 0, D_0, \ldots, D_{15}, P, 0, \ldots, D_{N_k-1},\\ &\quad \mathrm{Im}\{P\}, D_{N_k-1}, \ldots, 0, P, D_{15}, \ldots, D_0, 0], \quad (21)\\ \mathbf{X}^2 &= [0, P, D_0, \ldots, D_{15}, 0, P, \ldots, D_{N_k-1},\\ &\quad 0, D_{N_k-1}, \ldots, P, 0, D_{15}, \ldots, D_0, P]. \quad (22)\end{aligned}$$

At the receiver after the FFT operation, the received signal in frequency domain for the ZCP system can be given as

$$\begin{aligned}R_p^{\rho} &= Y_p^{1,\rho} + Y_p^{2,\rho} + W_p^{\rho}\\ &= H_p^{1,\rho}X_p^1 + H_p^{2,\rho}X_p^2 + W_p^{\rho} \quad (23)\end{aligned}$$

where R_p^{ρ} are the received signals of comb pilot system, $p = (0, 1, \ldots, \frac{1}{2}N_p - 1) \times (\frac{2(N+N_p)}{N_p})$ denotes the index of position of pilot in the first transmitter.

In order to avoid the interference from MIMO-PLC channel, only one pilot can go through the channel at the same time. The other adjacent transmitter must send zero data. The CFR matrix for the ZCP system can be written as when $X_p^1 = P$,

$$\begin{aligned}\tilde{H}_p^{1,\rho} &= \frac{R_p^{\rho}}{X_p^1}\\ &= \frac{H_p^{1,\rho}X_p^1 + 0 + W_p^{\rho}}{X_p^1}\\ &= H_p^{1,\rho} + \frac{W_p^{\rho}}{X_p^1};\end{aligned} \quad (24)$$

when $X_z^2 = P$,

$$\tilde{H}_z^{2,\rho} = H_z^{2,\rho} + \frac{W_z^{\rho}}{X_z^2}; \quad (25)$$

where z is the index of position of pilot in the second transmitter data. To completely eliminate the influence of pilot interference on the system, when subcarrier p transfer X_p^1, X_p^2 should be zero. In general, when subcarrier z transmits X_z^2, X_z^1 should be zero.

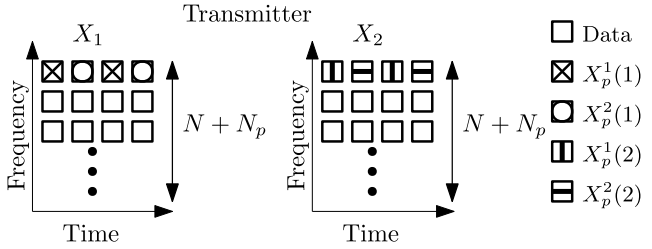

FIGURE 8. NZCP model.

In the 2×2 MIMO systems, in order to solve for the two unknown channel gains we need two equations. In the ZCP method, this achieved by inserting zeros in pilot subcarriers of adjacent MIMO channels. Pilot contamination will result in an underdetermined system of equations with four unknown variables and only two equations to solve the problem. The proposed NZCP method to estimate the channel interference is presented next.

IV. PILOT IMPROVEMENT

A. NONZERO-COMB PILOT

To solve the 2×2 system of equations in (15) for the four unknown channel gains, $H_p^{1,\rho}$ and $H_p^{2,\rho}$, $\rho = \{1, 2\}$, with one received OFDM symbol is impossible, since the system is underdetermined. To overcome this problem, we assume the channel is static over two received OFDM symbols and use two subsequent received symbol vectors to solve (15), that is

$$R_p^{\rho}(\zeta) = H_p^{1,\rho}X_p^1(\zeta) + H_p^{2,\rho}X_p^2(\zeta) + W_p^{\rho}(\zeta), \quad (26)$$

where R_p^{ρ} is the received OFDM signals, $\zeta = \{1, 2\}$ denotes the OFDM symbol index. The proposed NZCP system model with a the pilot spacing of 8 can be seen in Fig. 8, where the number of pilot subcarriers is $N_p = 512$, and total number

of subcarriers is $N + N_p = 4608$. It can be shown that the estimated CFR matrix of MIMO-PLC in NZCP system can be computed as

$$\tilde{H}_p^{1,\rho} = H_p^{1,\rho} - V^{1,\rho} = \frac{R_p^{\rho}1X_p^2(2) - R_p^{\rho}(2)X_p^2(1)}{X_p^1(1)X_p^2(2) - X_p^2(1)X_p^1(2)}, \quad (27)$$

$$\tilde{H}_p^{2,\rho} = \frac{R_p^{\rho}(1)X_p^1(2) - R_p^{\rho}(2)X_p^1(1)}{X_p^2(1)X_p^1(2) - X_p^1(1)X_p^2(2)}. \quad (28)$$

The derivation of (27) and (28) is presented in detail in Appendix B.

The NZCP approach requires the following condition, which is necessary to avoid a zero in the denominator of (51), i.e.

$$X_p^2(1)X_p^1(2) \neq X_p^1(1)X_p^2(2). \quad (29)$$

As the OFDM symbol in the frequency domain is complex-valued, we need to consider both the real and imaginary parts of the pilot symbols. Thus, we can rewrite (22), the condition of the pilot design as

$$\mathrm{Re}\{X_p^2(1)X_p^1(2)\} \neq \mathrm{Re}\{X_p^1(1)X_p^2(2)\}, \quad (30)$$

$$\mathrm{Im}\{X_p^2(1)X_p^1(2)\} \neq \mathrm{Im}\{X_p^1(1)X_p^2(2)\}. \quad (31)$$

To improve the SNR and thus the channel estimation and BER performance, it is advantageous to use for pilots QAM constellation symbols that are the farthest away from the origin (0,0), as they have the highest energy. To achieve this, all pilots are selected as

$$X_p^1(1) = X_p^2(1) = X_p^1(2) = -X_p^2(2) = (\sqrt{M} - 1)(1 + j), \quad (32)$$

where M denotes the order of QAM and $j^2 = -1$. It is worth noting that $X_p^2(2) = -(\sqrt{M} - 1)(1 + j)$ so that the condition is met (29).

Compared to the ZCP, the NZCP method does not need zero-pilot symbols to avoid channel interference from adjacent MIMO pilots. Therefore, for the same pilot-symbol spacing, NZCP can transmit additional information symbols on all of the zero-symbol pilot positions of ZCP, which in turn improves channel capacity. Furthermore, since in the NZCP approach the CFR is estimated by involving two OFDM symbols, the impact of the noise is averaged, thus, both the MSE and BER performances are significantly improved too.

B. AVERAGING AND MEAN SQUARE ERROR (MSE)

The CFR estimation, and thus the BER, can be greatly improved by averaging the effect of the noise. In this section, we introduce the proposed averaging approach shown in Fig. 9. For the first OFDM symbol, $\delta = 0$, and for each non-pilot subcarrier, n, we initialize the CFR averaging as

$$\hat{H}_n(\delta) = \tilde{H}_n(\delta). \quad (33)$$

For subsequent iterations, when $\delta = 2, \ldots, N_f - 1$,

$$\hat{H}_n(\delta) = a\tilde{H}_n(\delta) + (1 - a)\hat{H}_n(\delta - 1), \quad (34)$$

where $\hat{H}_n$ is the estimated CFR using the averaging method, $\tilde{H}_n$ is the estimated CFR at each OFDM symbol. $a \in (0, 1)$ is a weight factor and N_f is the frame size, which is the times of the averaging procession.

The MSE denotes the difference between the perfectly known CFR, H_n, and the estimated CFR, $\hat{H}_n$. It can be given as

$$MSE = 10\log_{10}\left(\frac{1}{N}\sum_{n=0}^{N-1}\left|H_n - \tilde{H}_n\right|^2\right) \text{ dB}, \quad (35)$$

where MSE is given in dB, is the prefect CFR. According to Eqs. (18), (24), (27) and (35), the MSE of each different channel estimation method can be calculated as follows:

- The Block pilot MSE:

$$MSE_{\text{block}} = 10\log_{10}\left(\frac{1}{N}\sum_{n=0}^{N-1}\left|\frac{W_k^{\tau,\rho}}{X_n^{\tau,\rho}}\right|^2\right) \text{ dB}, \quad (36)$$

- The ZCP MSE:

$$MSE_{\text{comb}} = 10\log_{10}\left(\frac{1}{N}\sum_{n=0}^{N-1}\left|\frac{W_n^{\rho}}{P}\right|^2\right) \text{ dB}, \quad (37)$$

- The NZCP MSE:

$$MSE_{\text{nz}} \quad (38)$$

$$= 10\log_{10}\left(\frac{1}{N}\sum_{n=0}^{N-1}\left|\frac{W_n^{\rho}(1) + W_n^{\rho}(2)}{2P}\right|^2\right) \text{ dB}, \quad (39)$$

  where $X_n^{\tau,\rho}$ denotes the values of the block pilots and P is the value of comb pilot. The derivation of (39) is presented in Appendix C.

By utilizing averaging, the the noise in each subcarrier is reduced with increasing number of transmitted OFDM symbols.

V. NUMERICAL RESULTS

In this section, we numerically evaluate the performance of the channel estimation with two pilot design approaches, i.e. block pilot [24] and comb pilot [25]. For the simulations we utilize a 2 × 2 MIMO-PLC channel model, with four different multipaths per link. The CIR and CFR for this channel are shown in Figs. (3) and (4). Furthermore, the performance of NZCP has been demonstrated to give a better BER results than the block/comb pilot approaches. Finally, the MSE results of various channel estimation methods have been computed as a function of SNR. At the receiver, we consider MMSE detection. The MMSE Equalizer coefficient is computed as

$$\mathbf{C}_n^{\text{MMSE}} = \frac{\mathbf{H}_n^{\dagger}}{\mathbf{H}_n\mathbf{H}_n^{\dagger} + \frac{1}{\gamma_s}\mathbf{I}^{2\times 2}}, \quad (40)$$

where $\mathbf{H}_n$ is the channel frequency response matrix of 2 × 2 MIMO-PLC system, † denotes the Moore-Penrose inverse of the matrix, $\mathbf{I}$ indicates the 2 × 2 unit matrix and γ_s represents the linear signal-noise-ratio.

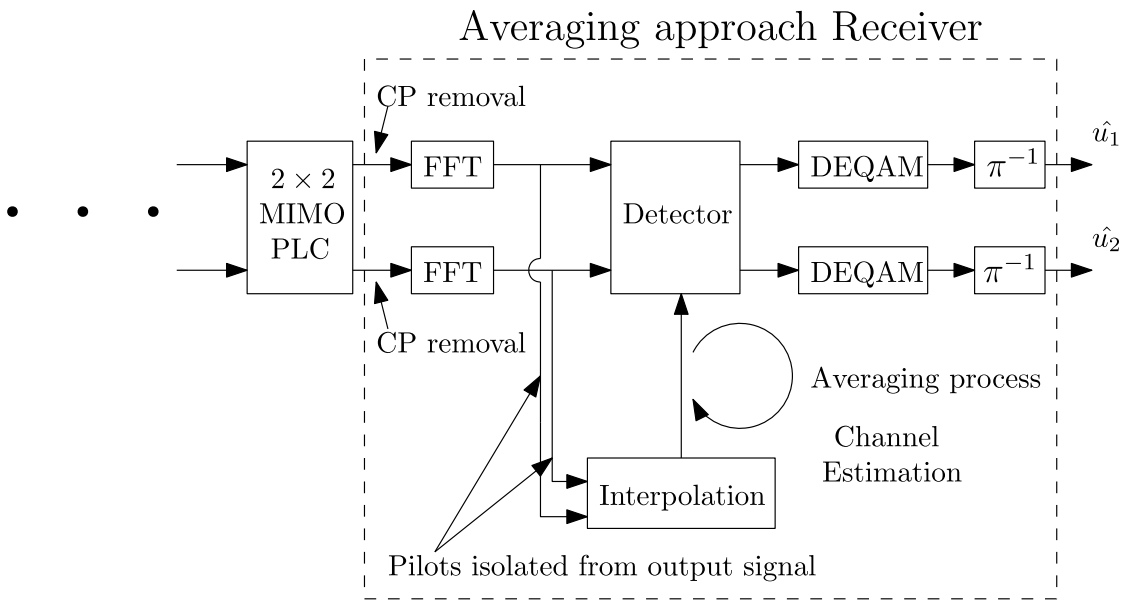

FIGURE 9. Comb/Block pilot system model using averaging.

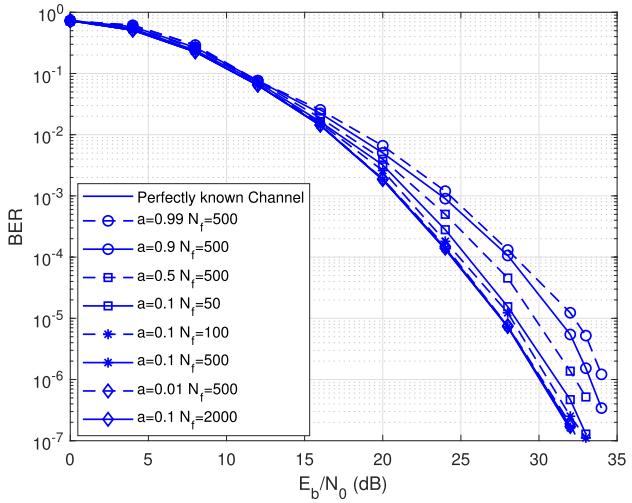

FIGURE 10. BER performance using NZCP with averaging method for uncoded systems.

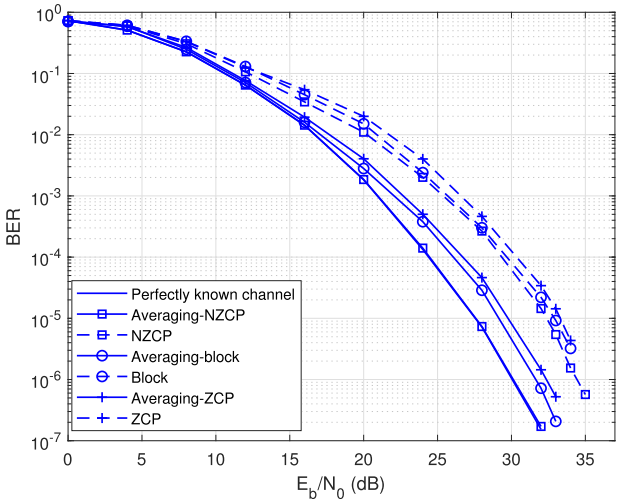

FIGURE 11. BER performance comparison of different channel estimation methods for uncoded systems.

A. CHANNEL ESTIMATION METHOD FOR UNCODED SYSTEMS

The performance of the proposed averaging method is controlled by the selection of the weight factor, a, and the number of transmitted OFDM symbols, N_f, used in computing the average. Fig. 10 displays the BER vs. E_b/N_0 performance by using different N_f and a values for the averaging NZCP system. The MMSE equalizer is constructed by using the perfect channel state information (CSI), which implies perfectly known PLC CFR from (3) and knowledge of the noise variance. With 500 frames, the BER performance is getting better when the weight factor decreases from 0.9 to 0.1. Moreover, the 0.1 weight factor has been kept in the simulation, the BER performance is getting better as the number of frame increased from 50 to 500 which can be seen in fig. 10 as well. it is worth noting that when the system changes to be 2000 frames, the BER performance has no difference compare with that of 500 frames. In other words, the averaging method in 500 times averaging is enough to adjust the impact of the noise in the MIMO-PLC channel estimation system. The following simulation about other types of the channel estimation methods are all under the 0.1 weight factor and 500 frames to investigate the BER performance and the MSE results.

As it can be seen in Fig. 11, the BER performance of the proposed NZCP methods outperforms both ZCP and block

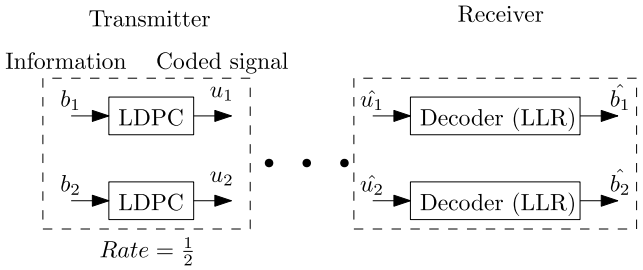

FIGURE 12. Coded system model.

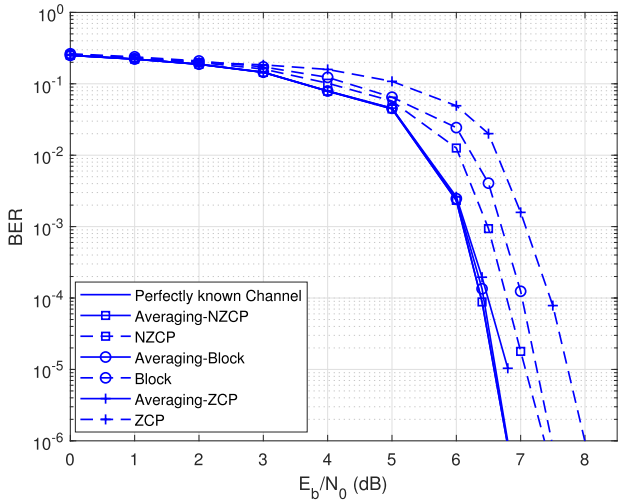

FIGURE 13. BER performance comparison of channel estimation methods with/without averaging over AWGN.

pilot approaches. This also the case when averaging is utilized to improve performance against AWGN and SαS. At a BER of 10^{-5}, there is approximately 0.5 and 1 dB improvement in E_b/N_0 between the NZCP and the block and comb pilot approaches, respectively. Using averaging further improves performance, for instance at a BER of 10^{-5}, there is an improvement in E_b/N_0 of 5 dB against the 1st iteration of NZCP and 3.6 and 4 dB against ZCP and block approaches, respectively, that also use averaging process. These results demonstrate that the proposed averaging channel estimation method can improve the channel estimation (in all methods) performance and in turn the BER. It is worth noting that $a = 0.1$ and $N_f = 500$ were used in the simulations. With these values the averaging NZCP approach achieves near perfect channel estimation that the block and comb pilot approaches fail to attain.

B. CHANNEL ESTIMATION METHOD FOR CODED SYSTEMS

In this paper, LDPC error correction coding is used to further improve the BER performance. We utilize a code rate $\frac{1}{2}$ and Gallager-type random construction for the LDPC code. The size of the sparse parity check matrix, $\mathbf{H}_{\text{LDPC}}$ is of dimensions 4096×8192. At the receiver end, the LDPC decoder shown in Fig. 12, computes the Log Likelihood Ratios (LLR) from

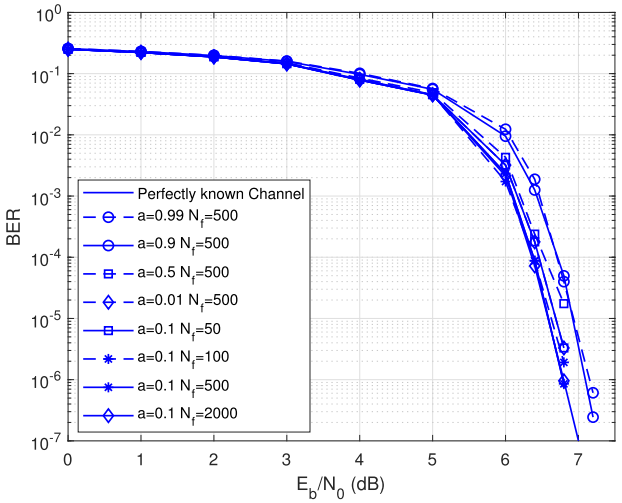

FIGURE 14. The effect of different weight factors and frame size for NZCP on the BER performance.

the soft QAM demodulated received symbol and converted back to binary data for detection.

As expected, it can be seen in Figs. 13 and 14, that the BER performances improve significantly against the uncoded systems. At a BER level of 10^{-5}, the proposed averaging NZCP method outperform the alternative approaches and matches the BER using the perfect channel CFR. The improvement in performance is approximately 20 dB in E_b/N_0 against the uncoded system. At a BER of 10^{-5}, there is an improvement in E_b/N_0 of 0.4 dB against the 1st iteration of NZCP and 0.5 and 0.8 dB against Block and ZCP approaches by using averaging process. Fig. 14 investigates the effect of a and N_f on the BER performance. It is evident from the figure that the introduction of LDPC codes in the system reduces the sensitivity of BER to both a and N_f. A setting of $a = 0.1$ and $N_f = 50$ provide a good compromise between performance and computational complexity.

C. MSE OF CFR IN DIFFERENT METHOD OF CHANNEL ESTIMATION

Fig. 15 shows the *MSE* of each different weight factor and frames in NZCP model, giving a more intuitive comparison of the difference between the perfect CFR and estimated CFR. The average MSE, MSE_{av}, is first computed against all nonpilot subcarriers and then averaged over N_f frames, i.e.

$$MSE_{av} = \frac{1}{N_f} \sum_{\delta=0}^{N_f-1} MSE_{\delta}. \tag{41}$$

The smaller the values of the MSE_{δ} and MSE_{av} are, the smaller the difference between perfect CFR and estimated CFR becomes. In other words, the pilot method that achieves the lowest MSE_{av} exhibits the best BER performance. In Fig. 15, with $a = 0.1$ weight factor and $N_f = 2000$ frame, the system can attain the best BER performance.

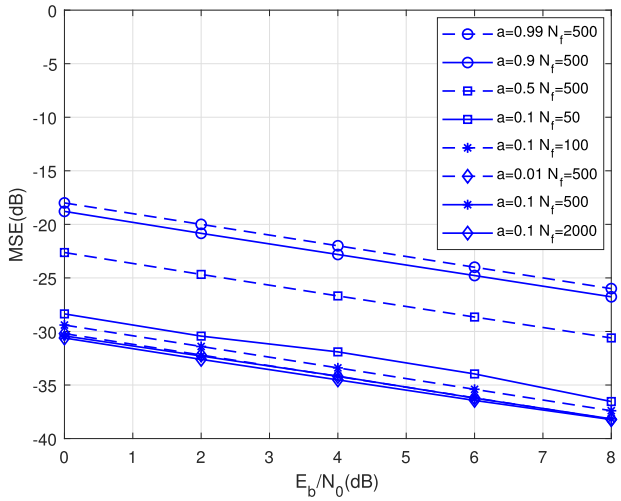

FIGURE 15. The MSE vs. E_b/N_0 of NZCP with averaging for different weight factors and frame sizes.

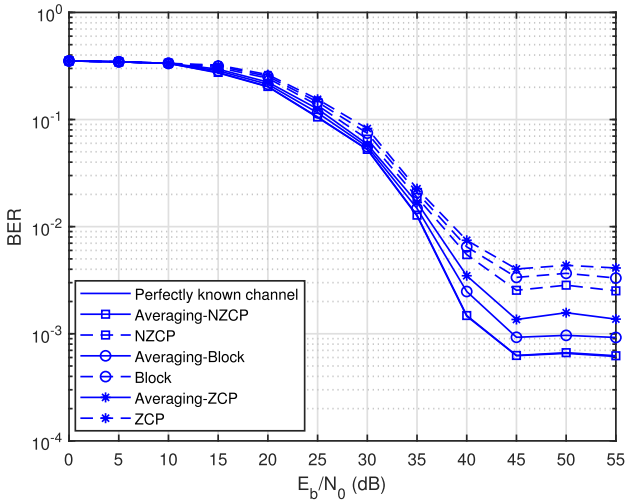

FIGURE 17. BER performance comparison of channel estimation methods with/without averaging over SαS noise with $\alpha = 1.5$.

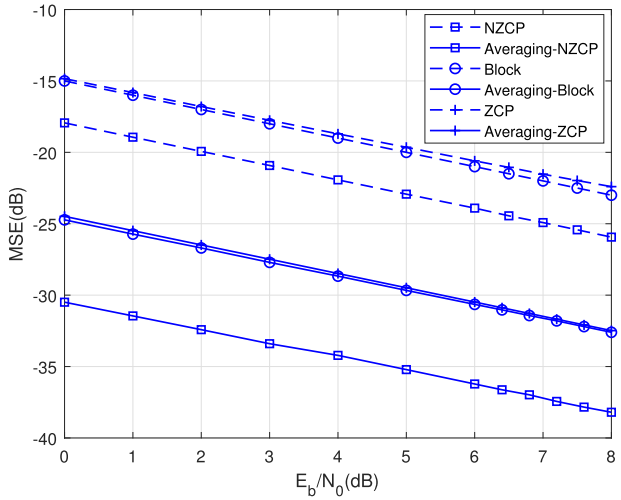

FIGURE 16. The MSE vs. E_b/N_0 for different pilot design systems over AWGN.

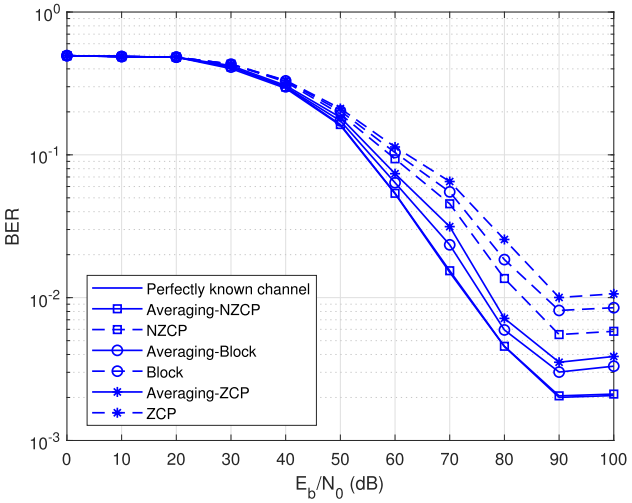

FIGURE 18. BER performance comparison of channel estimation methods with/without averaging over SαS noise with $\alpha = 1$.

Fig. 16, shows a comparison of MSE_{av} vs.E_b/N_0 for all the channel estimation methods considered in this paper. It is evident that the value of MSE_{av} decreases with increasing E_b/N_0. At an E_b/N_0 level of 8 dB, the averaging NZCP approach outperforms all other methods by at least 6 dB. It is worth noting that a and N_f were set to 0.1 and 2000.

D. CHANNEL ESTIMATION METHOD FOR CODED SYSTEMS OVER SαS IMPULSIVE NOISE

In this part, we investigate the impact of the SαS impulsive noise on the performance of the MIMO-PLC system for different values of α.

As it can be seen in Figs. 17 and 18, the BER performance over the MIMO-PLC system is worse than over the AWGN channel. With $\alpha = 1.5$, when SNR is 45 dB, the BER performance of the system using averaging NZCP is 6×10^{-4}, which is almost same as the BER performance when the perfectly known CFR is utilized. When $\alpha = 1$, the SαS impulsive noise exhibits as Cauchy distribution. As expected, it can be seen in Fig. 18 that the BER performance deteriorates and 2×10^{-3} is only achieved at 90 dB SNR. It is worth noting that the proposed averaging-NZCP system still matches the performance of the perfectly know CFR.

In Fig. 19, we investigate the performance improvement obtained by utilizing a hardlimiter at the output of the FFT block to limit the effects of the SαS noise. The function of the hardlimiter used is given as

$$f(x) = \begin{cases} +K, & \text{for } x \geq K \\ -K, & \text{for } x < -K \end{cases} \tag{42}$$

where x is the real or imaginary part of the FFT output and K is the threshold. For 16-QAM, a value of $K = 3.02$ was selected for a constellation with $\pm3\pm3j$ as outer constellation

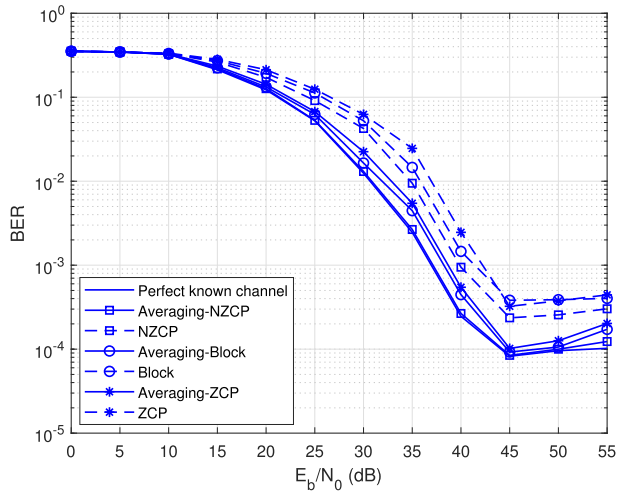

FIGURE 19. BER performance comparison of channel estimation methods with/without averaging over SαS noise with $\alpha = 1.5$ utilizing a hardlimiter.

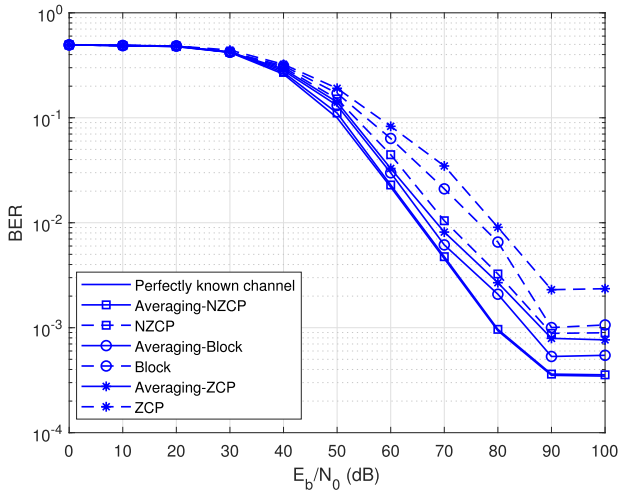

FIGURE 20. BER performance comparison of channel estimation methods with/without averaging over SαS noise with $\alpha = 1$ utilizing a hardlimiter.

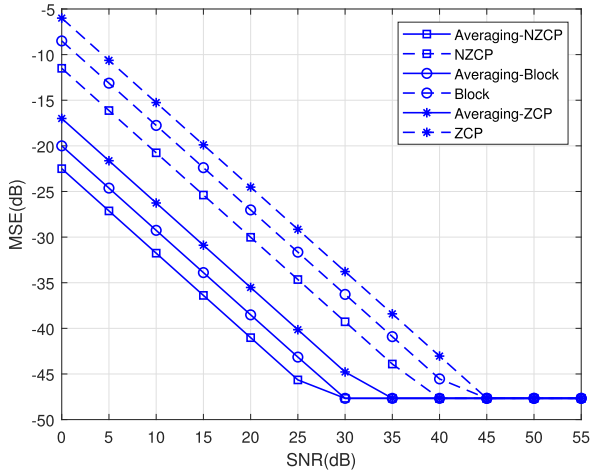

FIGURE 21. The MSE vs. E_b/N_0 for different pilot design systems over SαS noise with $\alpha = 1.5$.

points. A closer look at the results in Fig. 19 reveals that the BER performance has degraded compared to AWGN and is 8×10^{-5} at 45 dB, and matches the performance of

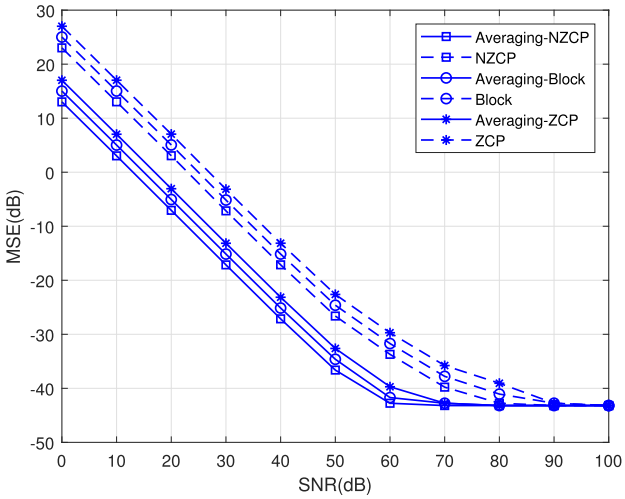

FIGURE 22. The MSE vs. E_b/N_0 for different pilot design systems over SαS noise with $\alpha = 1$.

the perfectly known CFR. Furthermore, the introduction of the hardlimiter is improves the performance when $\alpha = 1$. This is demonstrated in Fig. 20, where at at an SNR level of 90 dB, the BER performance is 2×10^{-3} and 3.5×10^{-4} without and with the hardlimiter, respectively, for the perifectly known CFT. It is worth highlighting that the proposed averaging-NZCP matches this performance too, whole outperforming the other methods.

Figs. 21 and 22 demonstrate the MSE performance over $\alpha = 1.5$ and $\alpha = 1$. In both cases of α, it can be seen from the figures that the proposed averaging NZCP outperforms the other pilot approaches, however, there is a 30 dB degradation in SNR for the error floor performance when $\alpha = 1$. It is worth noting that these results were obtained without the hardlimiter. It was found that although the introduction of the hardlimiter benefited the BER results, it had limited effect on the MSE performance.

VI. CONCLUSION

This paper has proposed an efficient averaging NZCP design for channel estimation in a 2×2 MIMO-PLC system utilizing real-valued OFDM symbols. The proposed approach can reduce the number of pilots required to half and achieve lower MSE compared to the ZCP and block pilot approach. The averaging method can be also utilized in the block and ZCP approaches resulting in a significant reduction of the impact of AWGN and SαS noise in the MIMO coded-PLC system. Simulation results demonstrate an improvement in BER performance in both uncoded and coded systems. Future work will investigate the performance of the proposed channel estimation in systems that employ precoding at the transmitter and under different impulsive noise environments. Although the proposed NZCP channel estimation method for MIMO can be easily extended to utilize more transmitters and receivers in wireless channels by extending the number of

transmit frames, in practical PLC channels there are limitations due to the physical number of wires available, and thus, it is not feasible to consider it in this study as we concentrated in 2-phase systems. For a 3-phase system it is possible to implement 3×3 MIMO and this is currently pursued in our research and will be subject of future publications. The main limitation is the availability of accurate channel models for the 3×3 MIMO-PLC systems.

APPENDIX A
DERIVATION OF THE CIR

For $q = 1$, we consider first the attenuation portion of the PLC CFR, which corresponds to the following analytic and bandlimited frequency response, i.e. $A(f) = 0, \forall f < 0$, and

$$A(f) = e^{-a_0 d_i} e^{-a_1 d_i f}, \text{ with } 0 \le f \le B$$

The inverse Fourier transform (FT) of $A(f)$ is computed as [30]

$$\begin{aligned} a(t) &= \int_{-\infty}^{\infty} A(f) e^{j2\pi ft} df \\ &= \int_0^B e^{-a_0 d_i} e^{-a_1 d_i f} e^{j2\pi ft} df \\ &= e^{-a_0 d_i} \int_0^B e^{-(a_1 d_i - j2\pi t)f} df \\ &= e^{-a_0 d_i} \frac{e^{-(a_1 d_i - j2\pi t)f}}{a_1 d_i - j2\pi t}\Big|_B^0 \\ &= \frac{1}{a_1 d_i - j2\pi t}\left(1 - e^{-a_1 d_i B} e^{e^{-j2\pi Bt}}\right) \\ &= \frac{e^{-j\tan^{-1}\left(\frac{2\pi t}{a_1 d_i}\right)}}{\sqrt{(a_1 d_i)^2 + (2\pi t)^2}}\left(1 - e^{-a_1 d_i B} e^{-j2\pi Bt}\right) \end{aligned} \quad (43)$$

It is worth noting that t here denotes the multipath delay spread of the PLC channel rather than time. We proceed to define $t_i = \frac{d_i}{v_p}$, then using the time-shift property of the FT [30], we can write

$$\begin{aligned} a(t - t_i)u(t - t_i) &= \int_0^B A(f) e^{-j2\pi f t_i} e^{j2\pi ft} df \\ &= \frac{e^{-j\tan^{-1}\left(\frac{2\pi(t-t_i)}{a_1 d_i}\right)}}{\sqrt{(a_1 d_i)^2 + [2\pi(t - t_i)]^2}} \\ &\quad \times \left(1 - e^{-a_1 d_i B} e^{-j2\pi B(t-t_i)}\right) \end{aligned} \quad (44)$$

where $u(t - t_i)$ is the Heaviside function delayed by t_i. The PLC CFR is analytic too and is given as

$$H_a(f) = \sum_{i=1}^{L} g_l e^{-a_0 d_i} e^{-a_1 f^k d_i} e^{-j2\pi f t_i} \quad (45)$$

The analytic CIR is obtained by taking the inverse FT of $H_a(f)$ as

$$h_a(t) = \int_{-\infty}^{\infty} H_a(f) e^{j\,2\pi ft} df$$

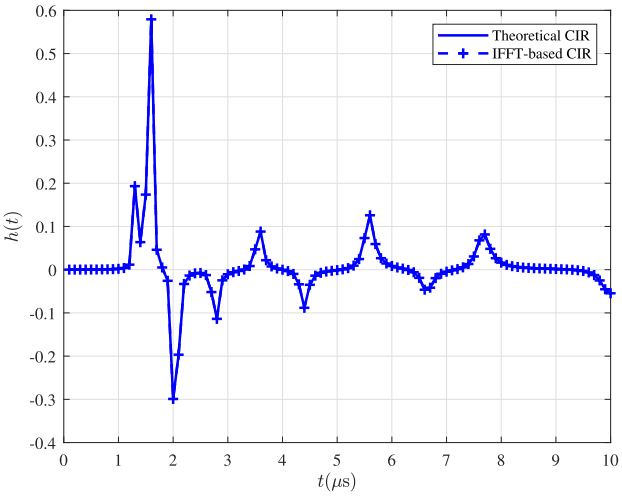

FIGURE 23. Theoretical and numerical CIR vs. multipath delay spread for a 15-path PLC multipath channel assuming a PLC channel bandwidth 20 MHz and truncated to 200 samples.

$$\begin{aligned} &= \int_{-\infty}^{\infty} \sum_{i=1}^{L} g_l e^{-a_0 d_i} e^{-a_1 f d_i} e^{-j2\pi f t_i} e^{j\,2\pi ft} df \\ &= \sum_{i=1}^{L} g_l e^{-a_0 d_i} \int_0^B e^{-a_1 f d_i} e^{-j2\pi f t_i} e^{j2\pi ft} df \\ &= \sum_{i=1}^{L} g_l e^{-a_0 d_i} a(t - t_i)u(t - t_i) \end{aligned} \quad (46)$$

The PLC CIR is obtained by taking the real part of $h_a(t)$, i.e.

$$\begin{aligned} h(t) &= \text{Re}\{h_a(t)\} \\ &= \sum_{i=1}^{L} g_l e^{-a_0 d_i} u(t - t_i) \\ &\quad \times \frac{\cos(\phi_i)[1 - e^{-a_1 d_i B}\cos(\theta_i)] + e^{-a_1 d_i B}\sin(\phi_i)\sin(\theta_i)}{\sqrt{(a_1 d_i)^2 + [2\pi(t - t_i)]^2}} \end{aligned} \quad (47)$$

where $\phi_i = \tan^{-1}\left(\frac{2\pi(t-t_i)}{a_1 d_i}\right)$ and $\theta_i = 2\pi B(t - t_i)$. Fig. 17 shows the theoretical energy-normalized CIR along with the one obtained by taking the inverse FT of the analytical CFR. Evidently, there is a very good agreement between the theoretical and numerically computed CIR. It is worth noting that closed-form solution may not exist for arbitrary values of q.

APPENDIX B
NONZERO CHANNEL ESTIMATION METHOD

According to (26), the perfect channel frequency response can be derived as

$$H_p^{1,\rho} = \frac{R_p^{\rho}(1) - H_p^{2,\rho} X_p^2(1) - W_p^{\rho}(1)}{X_p^1(1)}, \quad (48)$$

$$H_p^{2,\rho} = \frac{R_p^{\rho}(2) - H_p^{1,\rho} X_p^1(2) - W_p^{\rho}(2)}{X_p^2(2)}. \quad (49)$$

Combining (48) and (49), we can only solve for one of the unknown elements, i.e. the value of $H_p^{1,\rho}$, that is

$$H_p^{1,\rho} = \frac{R_p^{\rho}(1) - \frac{R_p^{\rho}(2) - H_p^{1,\rho} X_p^1(2) - W_p^{\rho}(2)}{X_p^2(2)} X_p^2(1)}{X_p^1(1)} - \frac{W_p^{\rho}(1)}{X_p^1(1)} \tag{50}$$

After straight forward mathematical manipulations, $H_p^{1,\rho}$ can be re-written as

$$H_p^{1,\rho} = \frac{R_p^{\rho}(1)X_p^2(2) - R_p^{\rho}(2)X_p^2(1)}{X_p^1(1)X_p^2(2) - X_p^2(1)X_p^1(2)} + V_p^{1,\rho}, \tag{51}$$

where $V_p^{1,\rho}$ represents the value of the noise part of the signal given as

$$V_p^{1,\rho} = \left| \frac{W_p^{\rho}(2)X_p^2(1) + W_p^{\rho}(1)X_p^1(1)}{X_p^1(1)X_p^2(2) - X_p^2(1)X_p^1(2)} \right|. \tag{52}$$

To estimate the CFR, the noise part in is ignored in (51), i.e.

$$\tilde{H}_p^{1,\rho} = H_p^{1,\rho} - V_p^{1,\rho} \tag{53}$$

$H_p^{2,\rho}$ is computed using a similar approach.

APPENDIX C
MSE OF NONZERO CHANNEL ESTIMATION

Using (35), (52) and (53), the MSE of the NZCP method can be given as

$$\begin{aligned} V_p^{1,\rho} &= |H_p^{1,\rho} - \tilde{H}_p^{1,\rho}| \\ &= \left| \frac{W_p^{\rho}(2)X_p^2(1) + W_p^{\rho}(1)X_p^1(1)}{X_p^1(1)X_p^2(2) - X_p^2(1)X_p^1(2)} \right|. \end{aligned} \tag{54}$$

Here, X_p represents the pilot symbols and can be replaced by P. Hence, (54) can be re-written as

$$\begin{aligned} \left| H_p^{1,\rho} - \tilde{H}_p^{1,\rho} \right| &= \left| \frac{W_p^{\rho}(2)P + W_p^{\rho}(1)P}{-PP - PP} \right| \\ &= \left| \frac{W_p^{\rho}(1) + W_p^{\rho}(2)}{2P} \right|. \end{aligned} \tag{55}$$

Combining (35) and (55), the MSE of NZCP method can be calculated using (39).

REFERENCES

[1] *IEEE Standard for Broadband Over Power Line Networks: Medium Access Control and Physical Layer Specifications*, Standard IEEE 1901, 2010.
[2] S. Zhang, C. Tsimenidis, H. Cao, and S. Boussakta, "Coded OFDM in PLC channels with SaS distribution impulsive noise using MRC detector," in *Proc. UK/China Emerg. Technol. (UCET)*, Aug. 2019, pp. 1–4.
[3] L. T. Berger, A. Schwager, P. Pagani, and D. M. Schneider, "MIMO power line communications," *IEEE Commun. Surveys Tuts.*, vol. 17, no. 1, pp. 106–124, 1st Quart., 2015.
[4] A. Schwager, D. Schneider, W. Baschlin, A. Dilly, and J. Speidel, "MIMO PLC: Theory, measurements and system setup," in *Proc. IEEE Int. Symp. Power Line Commun. Appl.*, Apr. 2011, pp. 48–53.
[5] S. Kasthala and G. K. D. P. Venkatesan, "Estimation of MIMO power line communication channel capacity using multi-conductor transmission line theory," in *Proc. 2nd Int. Conf. Appl. Theor. Comput. Commun. Technol. (iCATccT)*, 2016, pp. 787–792.
[6] F. Versolatto and A. M. Tonello, "A MIMO PLC random channel generator and capacity analysis," in *Proc. IEEE Int. Symp. Power Line Commun. Appl.*, Apr. 2011, pp. 66–71.
[7] B. Nikfar and A. J. H. Vinck, "Combining techniques performance analysis in spatially correlated MIMO-PLC systems," in *Proc. IEEE 17th Int. Symp. Power Line Commun. Appl.*, Mar. 2013, pp. 1–6.
[8] R. Hashmat, P. Pagani, A. Zeddam, and T. Chonave, "A channel model for multiple input multiple output in-home power line networks," in *Proc. IEEE Int. Symp. Power Line Commun. Appl.*, Apr. 2011, pp. 35–41.
[9] M. Almarashli and S. Lindenmeier, "Evaluation of vehicular 4G/5G-MIMO antennas via data-rate measurement in an emulated urban test drive," in *Proc. 48th Eur. Microw. Conf. (EuMC)*, Sep. 2018, pp. 300–303.
[10] D. Schneider, J. Speidel, L. Stadelmeier, and D. Schill, "Precoded spatial multiplexing MIMO for inhome power line communications," in *Proc. IEEE Global Telecommun. Conf.*, New Orleans, LA, USA, Nov. 2008, pp. 1–5.
[11] R. Hashmat, P. Pagani, A. Zeddam, and T. Chonavel, "MIMO communications for inhome PLC networks: Measurements and results up to 100 MHz," in *Proc. IEEE Int. Symp. Power Line Commun. (ISPLC)*, Rio de Janeiro, Brazil, Mar. 2010, pp. 120–124.
[12] B. Song, W. Zhang, and L. Gui, "Comb type pilot aided channel estimation in space time block coded OFDM systems," in *Proc. Int. Conf. Wireless Commun., Netw. Mobile Comput.*, 2005, pp. 202–206.
[13] W. Li, D. Qu, and T. Jiang, "An efficient preamble design based on comb-type pilots for channel estimation in FBMC/OQAM systems," *IEEE Access*, vol. 6, pp. 64698–64707, 2018, doi: 10.1109/ACCESS.2018.2877957.
[14] W. Hou, W. Ye, and S. Feng, "A channel estimation technique for MIMO-OFDM systems based on superimposed comb type pilot," in *Proc. Int. Conf. Wireless Commun., Netw. Mobile Comput.*, Sep. 2007, pp. 220–223.
[15] T. Shitomi, E. Garro, K. Murayama, and D. Gomez-Barquero, "MIMO scattered pilot performance and optimization for ATSC 3.0," *IEEE Trans. Broadcast.*, vol. 64, no. 2, pp. 188–200, Jun. 2018, doi: 10.1109/TBC.2017.2755262.
[16] F. Yang, P. Cai, H. Qian, and X. Luo, "Pilot contamination in massive MIMO induced by timing and frequency errors," *IEEE Trans. Wireless Commun.*, vol. 17, no. 7, pp. 4477–4492, Jul. 2018, doi: 10.1109/TWC.2018.2825982.
[17] L. Liu, T. Cheng, and Y. Luo, "Analysis and modeling of multipath for indoor power line channel," in *Proc. 10th Int. Conf. Adv. Commun. Technol.*, Feb. 2008, pp. 1966–1969.
[18] C. T. Mulangu, T. J. O. Afullo, and N. M. Ijumba, "Attenuation model for indoor multipath broadband PLC channels," in *Proc. IEEE-APS Topical Conf. Antennas Propag. Wireless Commun. (APWC)*, Sep. 2012, pp. 1084–1087.
[19] M. Zimmermann and K. Dostert, "A multipath model for the powerline channel," *IEEE Trans. Commun.*, vol. 50, no. 4, pp. 553–559, Apr. 2002.
[20] J. G. Gonzalez, J. L. Paredes, and G. R. Arce, "Zero-order statistics: A mathematical framework for the processing and characterization of very impulsive signals," *IEEE Trans. Signal Process.*, vol. 54, no. 10, pp. 3839–3851, Oct. 2006, doi: 10.1109/TSP.2006.880306.
[21] Z. Mei, M. Johnston, S. Le Goff, and L. Chen, "Finite length analysis of low-density parity-check codes on impulsive noise channels," *IEEE Access*, vol. 4, pp. 9635–9642, 2016, doi: 10.1109/ACCESS.2017.2649571.
[22] T.-T. Cao and Z.-W. Zheng, "Research on the non-blind channel estimation technologies for the MIMO-OFDM communication systems," in *Proc. Int. Conf. Electron., Commun. Control (ICECC)*, Sep. 2011, pp. 424–428.
[23] J.-S. Park, J.-K. Lee, and J.-U. Kim, "Block type pilot protection technique for clipping in OFDM systems," in *Proc. 9th Int. Conf. Adv. Commun. Technol.*, Feb. 2007, pp. 844–847.
[24] Z. Aida and B. Ridha, "LMMSE channel estimation for block—Pilot insertion in OFDM systems under time varying conditions," in *Proc. 11th Medit. Microw. Symp. (MMS)*, Sep. 2011, pp. 223–228.
[25] S. Elnoubi, S. Elbadawy, and C. Shaban, "Performance of turbo coded OFDM system with comb pilot channel estimation in Rayleigh fading channel," in *Proc. IEEE Mil. Commun. Conf. (MILCOM)*, Nov. 2008, pp. 1–6.
[26] J. Kim, J. Park, and D. Hong, "Performance analysis of channel estimation in OFDM systems," *IEEE Signal Process. Lett.*, vol. 12, no. 1, pp. 60–62, Jan. 2004.
[27] Z. Xakimjon and A. Bunyod, "Biomedical signals interpolation spline models," in *Proc. Int. Conf. Inf. Sci. Commun. Technol. (ICISCT)*, Nov. 2019, pp. 1–3.

[28] Y. Liao, Y. Hua, and Y. Cai, "Deep learning based channel estimation algorithm for fast time-varying MIMO-OFDM systems," *IEEE Commun. Lett.*, vol. 24, no. 3, pp. 572–576, Mar. 2020.
[29] R. Lavafi and B. Abolhassani, "A non-iterative channel estimation algorithm for mobile MIMO-OFDM systems with comb-type pilots," in *Proc. IEEE Int. Conf. Signal Process. Commun.*, Nov. 2007, pp. 380–383.
[30] A. Papoulis, *The Fourier Integral and its Applications*. New York, NY, USA: McGraw-Hill, 1962.

SHIRUI ZHANG received the B.Sc. degree in electrical and electronic engineering from Newcastle University, Newcastle Upon Tyne, U.K., in 2016, and the M.Sc. degree from the University of Southampton, Southampton, U.K., in 2017. He is currently pursuing the Ph.D. degree with the School of Electrical and Electronics Engineering, Newcastle University.

His research interests include power line communication for the smart grid, numerical and theoretical analysis of MRC detector in SISO-PLC channel systems, and MIMO-PLC channel estimations over uncoded and coded systems.

CHARALAMPOS C. TSIMENIDIS (Senior Member, IEEE) received the Ph.D. degree in communications and signal processing from Newcastle University, in 2002.

He is currently a Reader in digital communications with the School of Engineering, Newcastle University, and the Head of the Intelligent Sensing and Communications Group. He has published over 220 conference and journal articles, supervised successfully three M.Phil. and 50 Ph.D. students and made contributions in the area of arrayed receiver design for doubly-spread multipath fading channels to several U.K. and European funded research projects. His main research interests include adaptive array receivers for wireless communications, demodulation algorithms, error control and network coding, and protocol design for radio frequency, and underwater acoustic channels.

Charalampos C. Tsimenidis is a member of the IET.